

Machine learning-assisted quantification of organelle abundance.

Alexander James Long^{1,§}, Diogo Candeias^{2,3}, Nicki Frederick Coveña⁵, Luc Reymond⁶, Milena Schuhmacher⁷, Stephan Kemp⁴, Noémie Hamilton^{2,3}, and Triana Amen^{1,*}

¹School of Biological Sciences, University of Southampton, Southampton, UK

²Department of Biology, University of York, York YO10 5DD, United Kingdom

³York Biomedical Research Institute, Department of Biology, University of York, York, UK

⁴Laboratory Genetic Metabolic Diseases, Department of Laboratory Medicine, Amsterdam UMC, Amsterdam Gastroenterology Endocrinology Metabolism, University of Amsterdam, Amsterdam, The Netherlands

⁵Department of Complex Trait Genetics, Center for Neurogenomics and Cognitive Research, Amsterdam Neuroscience, Vrije Universiteit Amsterdam, Amsterdam, The Netherlands.

⁶Biomolecular Screening Facility, École Polytechnique Fédérale de Lausanne (EPFL), Lausanne, Switzerland

⁷Global Health Institute, Faculty of Life Sciences, Ecole Polytechnique Fédérale de Lausanne (EPFL), Lausanne, Switzerland

*For correspondence: t.amen@soton.ac.uk

§Technical contact: A.J.Long@soton.ac.uk

Abstract

Organelle abundance is a key microscopic readout of organelle formation and, in many cases, function. Quantification of organelle abundance using confocal microscopy usually requires estimating of their area based on the fluorescence intensity of compartment-specific markers. This analysis usually depends on a user-defined intensity threshold to distinguish organelle regions from the surrounding cytoplasm, which introduces potential bias and variability. To address this issue, we present a machine learning-assisted algorithm that allows for the quantification of organelle density using the open-source Fiji platform and WEKA segmentation. Our method enables the automated quantification of organelle number, area, and density by learning from training data. This standardizes threshold selection and minimizes user intervention. We demonstrate the utility of this approach for both membrane and non-membrane organelles, such as peroxisomes and stress granules, in human cells and whole fish samples.

Key features

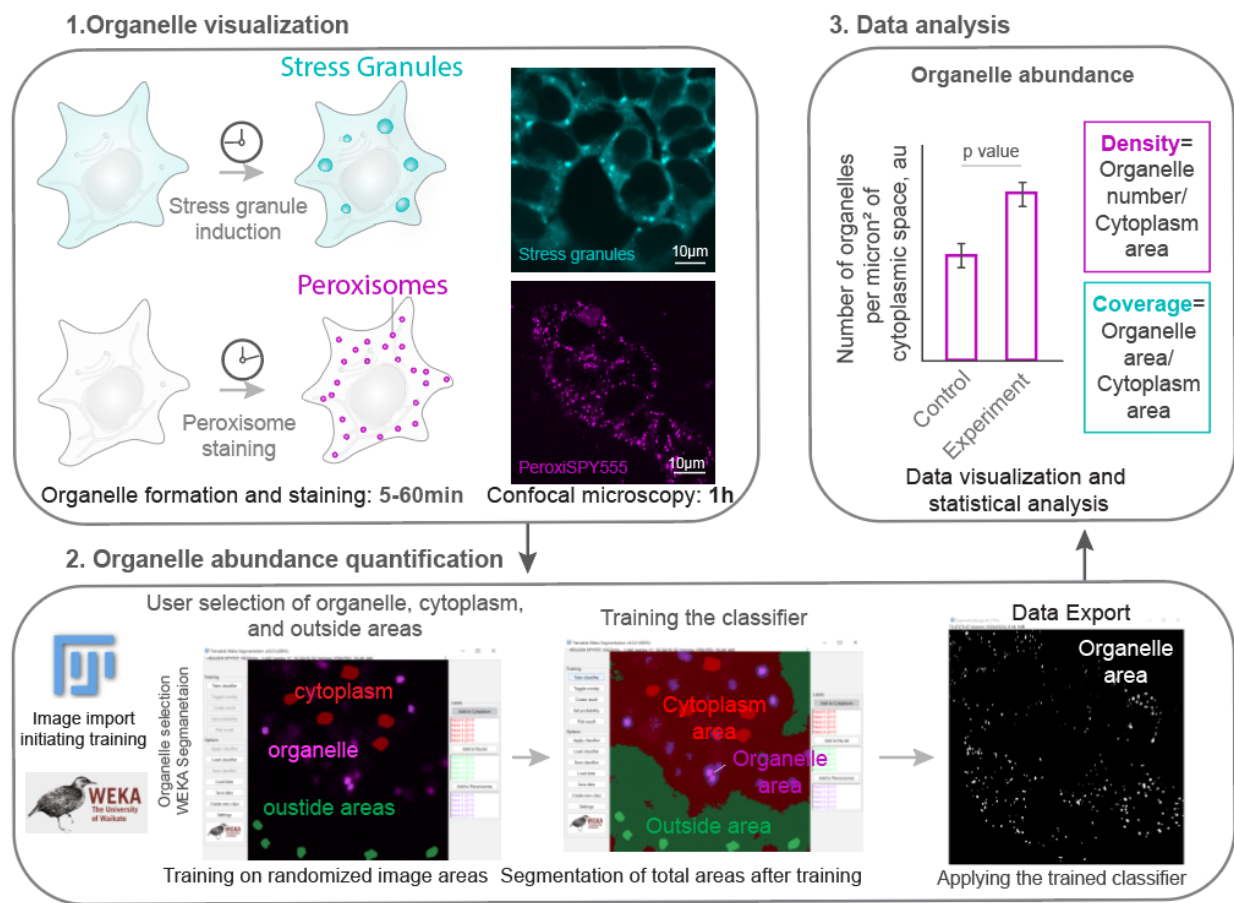
- The organelle abundance algorithm is an automated, open-source, Fiji-based tool that extracts the number and area of organelles and calculates organelle their abundance based on a single organelle marker.
- The macro measures the average intensity of all the segmented areas and quantifies their area.
- The algorithm is applicable to cellular compartments, including membrane-bound and membrane-less organelles.
- The training is performed on a sample dataset, enabling the algorithm to be applied to all images obtained with the same imaging parameters.

Keywords: organelle, peroxisome, stress granule, quantification, abundance, density, machine learning, Fiji, WEKA segmentation, PeroxiSPY

This protocol is used in: Journal of Cell Biology (2025), DOI: 10.1083/jcb.202505040

47
48
49

Graphical overview



50
51
52
53
54
55
56

Graphical overview of the protocol. Section 1 (Organelle visualization) corresponds with section A in the procedure. Section 2 (Organelle abundance quantification) corresponds with section B in the procedure. Section 3 (Data analysis) takes place after the procedure.

Background

57
58
59
60
61
62
63
64
65
66
67
68
69
70
71
72
73
74

Quantifying organelle abundance by determining how many organelles are present in the cell and the area of the cytoplasm they cover provides a useful measure of organelle dynamics and offers insight into organelle function. For example, stress granules are membrane-less organelles that form from stalled translation pre-initiation complexes and other proteins in response to stress (Ivanov et al., 2019; Protter and Parker, 2016; Riggs et al., 2020). They function when they form in the cytoplasm. Similarly, peroxisomes are membrane-enclosed organelles that are essential for lipid and oxidative metabolism (Kumar et al., 2024; Wanders and Waterham, 2006; Wanders et al., 2018). They undergo division and increase in number when their metabolic activity is required. In both cases, quantifying organelle density in the cytoplasm correlates with organelle function in healthy cells.

Organelle abundance can be estimated from confocal imaging by visualizing resident proteins or established organelle markers (Metz et al., 2017). An organelle marker is any fluorescently labeled molecule that localizes to an organelle. Examples include overexpressing a fluorescent protein fused to an organelle localization signal, or an endogenously tagged protein. Examples of endogenously tagged proteins include the CRISPR/Cas9 genomic fusion of polyA-binding protein PABPC1 to Dendra2, which is used as a marker of stress granules (Amen and Kaganovich, 2021), and ATP-binding cassette sub-family D member 3 (ABCD3) fused to GFP as a marker of peroxisomes (Borisyyuk et al., 2025). Other examples include using a fluorescent probe that selectively targets the organelle, such as PeroxiSPY, which is used to label peroxisomes (Korotkova et al., 2024), or using antibody staining of organelles post-fixation (Borisyyuk et

75 al., 2025). The quantification requires segmentation, or defining the boundaries of compartments, which is often based on
76 visual inspection. Manual segmentation is prone to error; for example, it is difficult to consistently outline highly variable,
77 punctate, or overlapping patterns. To improve the reliability of quantification, thresholding methods set an intensity value
78 independent of the user and improve consistency (Russell et al., 2009). Machine learning approaches further reduce errors
79 of manual segmentation by providing consistent labeling based on user-defined parameters (Arganda-Carreras et al., 2017;
80 Lam et al., 2025; Lefebvre et al., 2025).

81 Here we present a protocol for quantifying the abundance of membrane and membrane-less organelles based on a
82 single marker using Fiji software (Schindelin et al., 2012). This protocol combines the WEKA Segmentation (Arganda-
83 Carreras et al., 2017) and watershed algorithms into a user-friendly workflow. The quantification is based on trainable
84 organelle recognition, which limits user-defined thresholding bias and improves the consistency of image processing
85 (Isensee et al., 2021; Lefebvre et al., 2025; Newby et al., 2018). Recognition requires reliably outlining organelles for initial
86 training, a task that can be done by experienced researchers. The trained classifier can then be applied to any number of
87 images obtained with the same microscopy settings. Alternatively, a beginning researcher can train the classifier and include
88 controls to verify whether the recognized area corresponds to an organelle area.

89 As a proof-of-concept, we validate that machine learning-assisted recognition of cellular compartments
90 corresponds to an independent marker of cellular cytoplasmic and peroxisome areas, using a control marker for both the
91 organelle and the cytoplasm. In many experimental setups, adding additional markers is not feasible, and manually extracting
92 the cytoplasmic area from a single organelle marker is biased and time-consuming. Our results demonstrate that
93 machine-learning assistance enables the consistent and reliable identification of these regions. Finally, we apply the macro
94 to quantify the non-membrane compartment density of stress granules using a CRISPR/Cas9-tagged PABPC1 cell line
95 (Amen and Kaganovich, 2020). The algorithm recognizes conditions in which there are no stress granule compartments and
96 extracts areas based on a single marker.

97
98 This protocol can be modified further to estimate organelle coverage, the area of the cell occupied by the cytoplasm,
99 or to extract abundance in 3D using stacks of 2D images obtained from tissues. This provides a useful tool for quantitative
100 cell biology experiments.

101
102

103 **Materials and reagents**

104
105

106 **Biological materials**

107 **Cell lines and organisms used in this study**

- 108 1. Human embryonic kidney cells HEK293T (ATCC® CRL-3216™)
- 109 2. HEK293T PABPC1-DDR2 cell line (Amen and Kaganovich, 2021)
- 110 3. Zebrafish *Danio rerio*;

110

111 **Zebrafish husbandry and ethics:**

112 All zebrafish were raised at the University of York in UK Home Office approved aquaria and maintained following standard
113 protocol (Cunliffe, 2003). Tanks were maintained at 28 °C with a continuous re-circulating water supply and a daily
114 light/dark cycle of 14/10 hours. The nacre WT background strain was used to perform injections.

115

116 **Cell culture**

117 HEK293T cells were maintained in high-glucose DMEM media supplemented with 10% fetal bovine serum (FBS), 1%
118 penicillin/streptomycin, at 37 °C/5% CO₂. The media was replaced every 2nd day; the cells were seeded at a density of
119 50,000 cells per a well of a 4-well imaging plate. Cells were visualized at a 50-70% confluency, cells were split before they
120 reached 90% confluency.

121

122 **Stress granule formation**

123 To visualize stress granules, replace the media in the glass-bottom plate for live-cell imaging with 200 µM sodium arsenite
124 dissolved in the cell culture media and incubate for 1 h in the cell culture incubator at 37 °C/5% CO₂ (Amen and Kaganovich,
125 2020). To prepare 200 µM sodium arsenite, dissolve 2 µl of 100 mM sodium arsenite stock in water in 1 ml of media, use
126 vortex mixing or pipetting.

127

128 **Peroxisome staining**

129 Peroxisomes were stained with PeroxiSPY (Korotkova et al., 2024), as described in (Howman et al., 2025). To visualize

130 peroxisomes, replace the media in the glass-bottom plate for live-cell imaging with 1 μ M PeroxiSPY dissolved in the cell
131 culture media and incubate for 5-10 m in the cell culture incubator at 37 °C/5% CO₂.

132

133 Reagents

134

135 1. PeroxiSPY555 (Spirochrome, catalog or CAS number: SC207: Peroxi_SPY555). Store 1 mM stock in DMSO in -20 °C
136 long-term, aliquotes can be stored at +4 °C.

137 2. Sodium arsenite (Thermo Fisher Scientific, catalog or CAS number: 7784-46-5)

138 3. Immersion liquid (Cargille, catalog or CAS number: 16482)4. Penicillin/Streptomycin for cell culture (Pan Biotech,
139 catalog or CAS number: P06-07050)

140

141 Solutions

142

143 1. Dulbecco's Modified Eagle's Medium (DMEM) cell culture media with 10% fetal bovine serum (FBS) (Pan Biotech, P30-
144 3031, P04-03590)

145 2. 100 mM sodium arsenite in water (use as a 500x stock). To dissolve in tissue culture medium add 2 μ l of the stock to 1
146 ml of medium, mix by vortex mixing or pipetting before adding to the cells.

147 3. 1 μ M PeroxiSPY in DMEM medium. To dissolve PeroxiSPY in media, add 1 μ l of the 1 mM stock to an Eppendorf tube,
148 then add 1 ml of media and mix by vortex mixing or pipetting before adding to the cells.

149

150 Laboratory supplies

151

152 1. 4-chamber glass bottom plates CellVis, catalog number: D35C4200N, cover glass (0.13-0.16 mm), used for confocal
153 imaging

154 2. tissue culture 10 cm plates (Sigma) used for cell culture.

155 *Note: Plastic plate thickness will not allow 60x confocal imaging, however it is possible to image larger organelles through*
156 *the plastic plates with lower magnification e.g. 20x objective, e.g. they can be used for nuclei segmentation.*

157

158 Equipment

159

160 1. Nikon A1r confocal microscope (Nikon, A1r), equipped with a CFI Plan Apo Lambda 60x oil NA 1.42 objective

161 2. Nikon W1 Spinning disk microscope (Nikon), , equipped with a CFI Plan Apochromat Lambda S 60XC Sil objective

162 3. CO₂ chamber and temperature control unit (OKO Lab)

163 4. CO₂ incubator for cell culture (Thermo Fisher Scientific.)

164 5. CFI Plan Apo Lambda 60x oil NA 1.42 objective (Nikon)

165 6. 561 nm laser and a 488 nm laser (Coherent)

166 5. Eppendorf tubes (Eppendorf)

167

168

169
170
171

Software and datasets

Type	Software/dataset/resource	Version	Date	License	Access (free or paid)
Data	Example dataset	N/A	01.12.2025	N/A	Free, Supplementary Dataset S1
Software	Fiji software (or ImageJ)	Java 21.0.7 (64-bit)	01.12.2025	(Schindelin et al., 2012; Schneider et al., 2012)	Free
Software	NIS Nikon software	4.1	N/A	N/A	Paid (microscope software)
Macro (organelle abundance algorithm)	Resource	1.0	01.12.2025	N/A	Free, Supplementary Code S1

172
173
174
175

Procedure

A. Image acquisition and wet-lab component of the protocol

177 Cell culture preparation for live-cell imaging, timing: 24 h
178 To prepare for confocal imaging we used standard cell culture protocols. Cell lines were maintained in DMEM,
179 supplemented with 10% fetal bovine serum (FBS), 1% penicillin/streptomycin, at 37 °C/5% CO₂.

180 **Caution:** If your microscope detects the signal from phenol red in the media, use phenol red-free alternatives, e.g. P04-
181 01158 (Pan Biotech).

182 1. One day before image acquisition split the cells into a glass-bottom imaging plate to achieve a 50-60% confluency the
183 next day. We split HEK293T for peroxisome staining and HEK293T PABPC1-DDR2 for stress granule imaging at a density
184 of 50.000 cells per well of the microscopy plate.

185 2. Live-cell image acquisition, Timing: 1 h

186 Imaging organelles requires high spatial resolution. For this protocol we used Nikon A1r confocal microscope equipped
187 with a gallium arsenide phosphide cathodes (GaAsP) photomultiplier modules, a CO₂ chamber and a temperature control
188 unit. The imaging was done using a bi-directional Galvano-scanning mode using CFI Plan Apo Lambda 60x oil NA 1.42
189 objective, using a 561 nm laser (Coherent, 50 mW) for PeroxiSPY555, and 488 nm laser (Coherent, 50 mW) for DDR2.

190 2.1. Turn on the microscope, required lasers, and the CO₂/temperature units. Ensure that the CO₂ and 37 °C
191 temperature are stabilized for at least 15 minutes before the imaging.

192 2.2. Initiate the software and adjust the software parameters for acquisition. We used 0.5-2% laser power and HV
193 (gain) of 100 and acquired a 1024*1024 px, zoom 3-4x images.

194 **Note:** To ensure maximum resolution we recommend following Nyquist sampling (Shannon, 1949) – adjust the pixel size to
195 be 2.3 times smaller than the smallest compartment that you are imaging. Increasing HV (gain) will increase the brightness
196 but will also increase the noise. To ensure that data is usable, the same imaging parameters should be applied to all images
197 within one experiment. Any confocal microscope can be used for this protocol.

198 3. Staining and acquiring of the organelle images.

199 3.1. **Stress Granule imaging** requires inducing the formation of stress granules as previously described (Amen
200 and Kaganovich, 2020). Pipette a 100 mM sodium arsenite solution as a 1/500 part of your total media volume in
201 an empty Eppendorf tube, e.g. for 0.5 mL of media we pipette 1 µL of arsenite. Collect the media from the cells
202 and mix with sodium arsenite by vortex mixing or pipetting. After mixing, add the mix to the plate and incubate
203 for one hour in the cell culture incubator.

204 For **peroxisome imaging**, stain cells with PeroxiSPY for 10 m as previously described (Howman et al., 2025;
205 Korotkova et al., 2024) To incubate the cells with 1 µM of PeroxiSPY555 for 10 m: pipette a 1 mM PeroxiSPY
206 aliquot as a 1/1000 part of your total media volume in an empty Eppendorf tube, e.g. for 0.5 mL of media we
207 pipette 0.5 µL of PeroxiSPY. Collect the media from the chosen microscope plate and mix with PeroxiSPY by

208 vortex mixing or pipetting. After mixing, add the mix to the plate and incubate for 5-10 m.

209 **Caution:** Do not leave the cells without media for over 20 s to avoid osmotic stress. To achieve uniform staining and
210 organelle formation, all the media should be mixed with the molecules

211 3.2. Add immersion liquid to the objective (we use 60x oil objective) and position the plate. Adjust focus until the
212 cells are visible and in-focus. Randomly choose imaging area and adjust parameters of acquisition (e.g, HV-100,
213 Laser power = 1%, Zoom 3, 1024*1024 px, scan speed 1/2-1/4).

214 3.3. Acquire and save all images with accessible labels (we use .nd2 Nikon NIS Software), including cell line,
215 staining, genetic modification, treatment, and time if applicable.

216 **Pause point:** images can be stored and processed when needed.

217

218 B. Image analysis – quantification of organelle density

219 1. Training the classifier for organelle abundance quantification. A classifier is an algorithm or model used to classify data
220 (Bi et al., 2019). In the Fiji software this is stored as a “.model” file, and is used by the Trainable Weka Segmentation tool
221 to classify sections of an image into organelles, cytoplasm, and area outside of the cytoplasm.

222 1.1. Open the macro file in Fiji (Supplementary code S1), either by dragging the file onto the Fiji window, or by
223 clicking “File > Open” on the Fiji window.

224 1.2. Once the macro editor window appears, full screen the window and click “run” in the lower left corner.

225 1.3. Follow the prompt on the pop-up window. Type 1 in the dialog box to train a classifier from scratch, or type
226 0 to use a pre-trained classifier. If you type 0, skip to step 2.1

227 **Note:** to open .nd2 images you will need to install the .nd2 reader in Fiji ([https://imagej.net/ij/plugins/nd2-
228 reader.html](https://imagej.net/ij/plugins/nd2-reader.html))
229 1.4. Using the pop-up window, select the folder containing your training image, ensuring this folder
230 contains only the training image, and a folder in which to store the trained classifier and training data. Ensure that
231 this second folder is empty.

232 1.5. Wait for the macro to run until a small window titled “Select Identifiable Features” appears. Additionally, 2
233 other important windows will appear, titled “Trainable Weka Segmentation” (Arganda-Carreras et al., 2017) and
234 “Reference”.

235 1.6. Using the “Trainable Weka Segmentation” window, and the “Reference” window for clarity, draw around up
236 to 5 visible organelles, depending on how many are visible. Click the “Add to Organelles” button on the right of
237 the window before drawing around each subsequent one.

238 **Note:** peroxisomes are ~0.5µm round compartments in the cytoplasm that co-localize with peroxisome marker GFP-SKL in
239 healthy cells (Figure 2A). When drawing in Weka segmentation, only select the area that is peroxisomes, avoid overdrawing.

240 1.7. After selecting up to 5 visible organelles, select 5 sections of cytoplasm, each at least the size of the organelles
241 selected in step 1.6. Click the “Add to Cytoplasm” button on the right of the window before drawing around each
242 subsequent area.

243 1.8. Finally, select 5 sections outside of the cytoplasm, each at least the size of the organelles selected in step 1.6.
244 Click the “Add to Nuclei” button on the right of the window before drawing around each subsequent area.

245 1.9. Click the “OK” button in the “Select Identifiable Features” window and wait until the training has been
246 completed. To identify if the training has been completed, wait until the image displayed in the “Trainable Weka
247 Segmentation” window changes to highlight the organelles (purple), cytoplasm (red), and nuclei/background
(green).

248 1.10. A new window will appear, asking to continue or finish training. Type 1 into the dialog box to finish training,
249 and type 0 to continue training. We recommend repeating the training steps (steps 1.6-1.10) 9 additional times,
250 totaling 10 training loops. This number is based on data from Figure 2B, which suggests that after 10 training loops
251 the change in identified area was minimal.

252 2. Using the Macro to analyze an image. The macro will use the trained classifier (1.1-1.10) and a watershed function to
253 automatically determine the area and intensity of the visible organelles and cytoplasm, and the abundance of the visible
254 organelles.

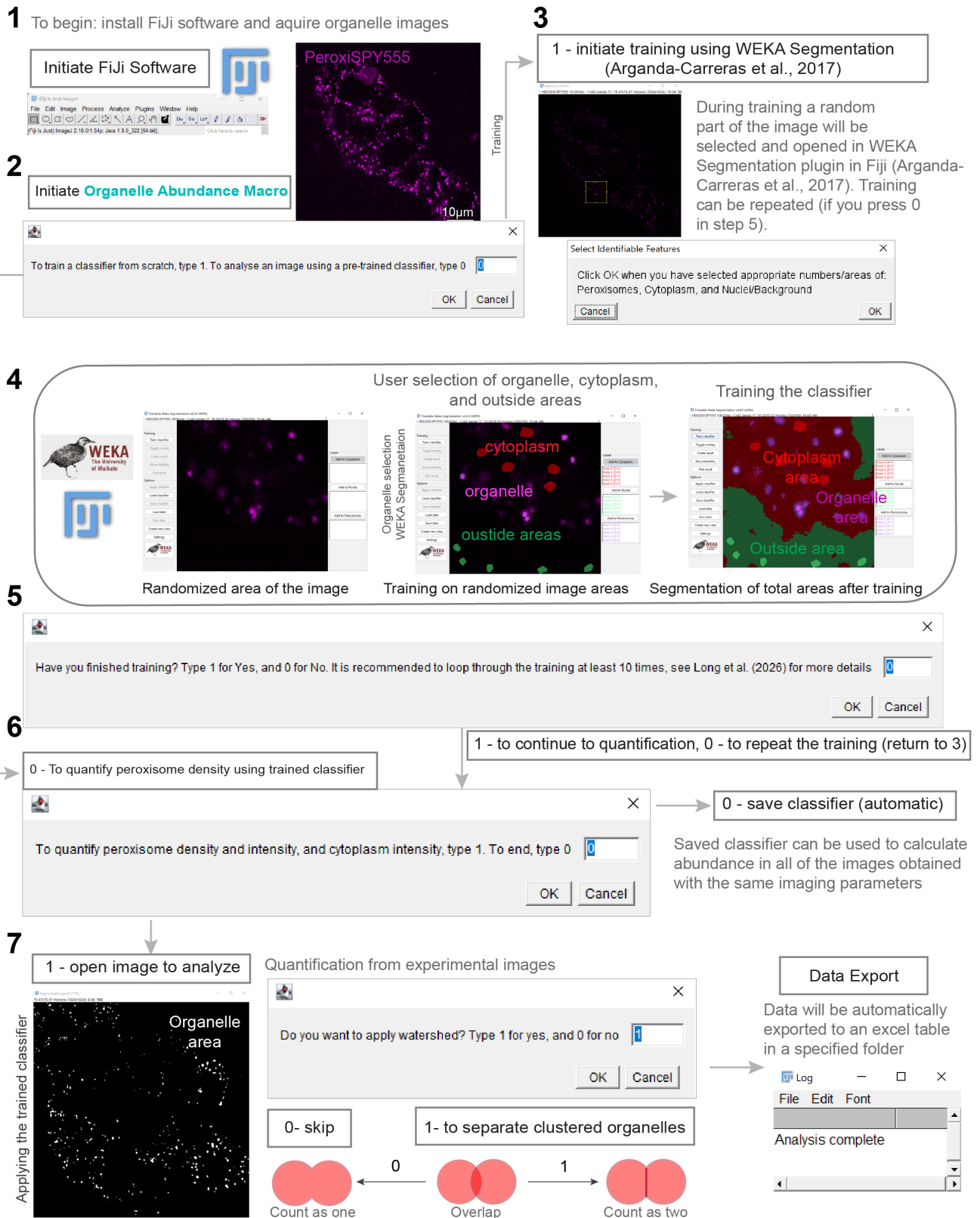
255 2.1. A pop-up window will appear asking whether you wish to analyze a new image using the previously trained
256 classifier. Type 1 to continue with organelle analysis, or 0 to stop the macro. Stopping the macro is recommended
257 if you wish to analyze more than one image. Typing 0 will result in the text “Training complete” being displayed.

258 2.2. In the next pop-up window titled “Select your Files”, select the folder containing the image you wish to
259 analyze. Ensure this folder contains only one image. Then select a folder to save the results, ensuring this folder is
260 empty.

261 2.3. This step is only applicable if you are using a pre-trained classifier (if steps 1.4 – 1.10 were skipped). The
262 same pop-up window described in step 2.3 will appear with an additional field. Select the folder which contains
263 the pre-trained classifier. This folder should contain 2 files in the form of a classifier file (ending in .model), and a

264 data file.
265 2.4. Wait for the analysis section of the macro to run until a pop-up window asks whether you want to apply Fiji's
266 watershed tool to the organelles. This will attempt to separate organelles that are too close, ensuring they are
267 counted separately. This is useful in samples with high organelle density; higher density of organelles increases
268 the likelihood of organelles overlapping and thus causing the macro to count fewer than are present in the image.
269 Type 1 for yes, and 0 for no.
270 2.5. Wait until the text "Analysis complete" displays in the "log" window.
271
272
273

Figure 1. Organelle abundance quantification using Fiji macro



274
275
276
277
278

Figure 1. Organelle abundance quantification workflow (Code S1). Figure numbers correspond with procedure steps: 1 is procedure section A, 2 is 1.1-1.3 in procedure section B, 3 is 1.4 in procedure section B, 4 is 1.5-1.9 in procedure section B, 5 is 1.10 in procedure section B, 6 is 2.1-2.3 in procedure section B, and 7 is 2.4 in procedure section B.

279
280

281 **Result interpretation**

282 Expected output from this protocol is an excel table with the list of detected organelles (Supplementary table 1), their areas
283 and corresponding average intensity per each area, with a calculated density of organelles in the cytoplasm in the form of
284 number of organelles per square micron (abundance). Results can be plotted as a distribution of organelle areas (Figure 2A)
285 or densities (Figure 3A). Coverage of the area can be extracted by dividing the sum of organelle areas by the sum of organelle
286 and cytoplasmic areas.

287 Image quality determines whether the data are usable and quantifiable. Image quality depends on the sample preparation
288 and correct microscopy settings. For each organelle we recommend consulting with the literature on the expected size and
289 number of the organelles in the cell line of choice. When imaging organelles for the first time, ensure that you have a verified
290 organelle marker as a control (Figure 2A). To ensure maximum resolution, adjust the microscope settings to ensure that the
291 pixel size is at least 2.3 times smaller than the smallest compartment that you are imaging. This can be done by increasing
292 the image size or physical zoom. Avoid saturation of the organelle areas and ensure that the background noise is minimized
293 by reducing the gain. The protocol estimates cytoplasmic areas based on the residual fluorescence, it is recommended to
294 confirm whether the cytoplasmic area corresponds to actual cytoplasmic area using secondary markers (Figure 2A).

295 It is recommended to perform at least three biological replicates to obtain the data. The same classifier can be used to
296 quantify the areas in all the images obtained with the same imaging parameters. Additionally, it is recommended to quantify
297 organelle areas in at least 100 cells per condition. If the data follows normal distribution, determined by Shapiro-Wilks test,
298 P values can be calculated by two-tailed Student's t test for two samples or one-way ANOVA for multiple samples. The
299 equality of variances can be verified by the Brown-Forsythe or F test. Mann-Whitney (two groups) or Kruskal-Wallis
300 (multiple groups) tests can be used for samples that do not follow a normal distribution. The sample sizes can be determined
301 using power analysis. Results obtained from the images with different microscopy parameters cannot be reliably
302 comparatively analysed (Figure 2C).

303 **Validation of protocol**

304 We confirmed that machine learning-assisted area segmentation corresponds to the physical cytoplasmic and organelle
305 space using secondary markers (Figure 2A). Peroxisomal area quantified using organelle abundance macro is the same as
306 a manually thresholded area defined by a GFP-SKL peroxisomal marker in the same cells (Figure 2A).

307 The segmentation relies on the intensity, therefore it is recommended to train the classifier for each set of imaging
308 parameters, such as laser power or exposure. It takes only 5-10 training cycles, using the random area of the same image
309 (Figure 1, Figure 2B), to reliably train the classifier. We showed that increased laser power corresponds to a gradual
310 increase in areas recognized by the classifier (Figure 2C), thereby requiring classifier training for each independent
311 dataset.

312 The classifier, once trained, can be applied to a necessary number of repeats of images obtained with the same microscope
313 settings, at least 3 biological replicates were done for the experiments presented here. We applied a stress granule trained
314 classifier to identify stress granule density in control and stress conditions (Figure 3A). The macro allowed extracting the
315 absence of stress granules from all the control images.

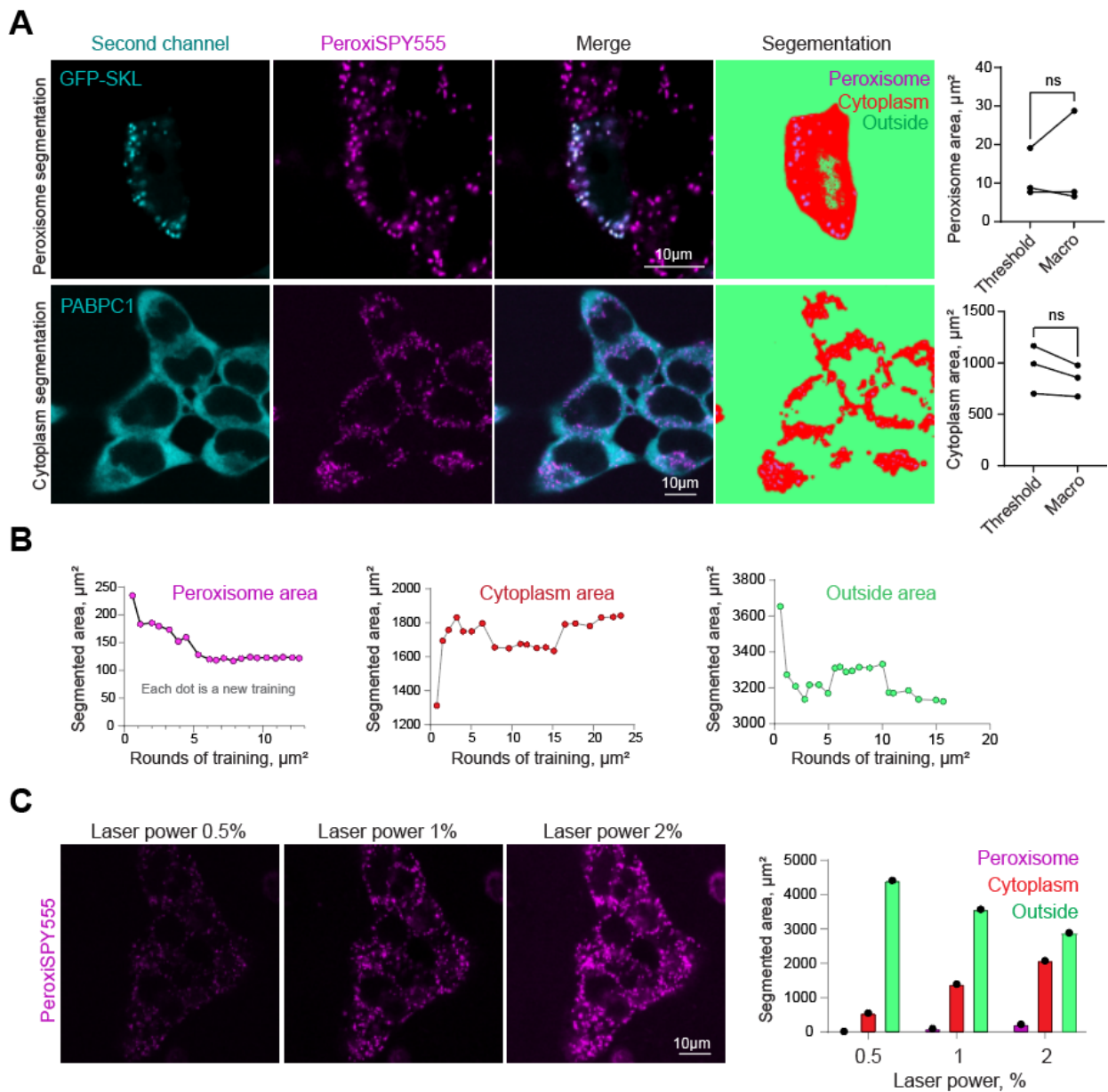
316 This tool extracts organelle abundance data from 2D images, 3D space abundance can be extracted from a Z-stack of 2D
317 images. Here we estimated peroxisome density in zebrafish *D. rerio* injected with PeroxiSPY peroxisome probes (Figure 3
318 B). Additionally, this protocol can be applied to other cellular organelles in different cell types, resulting in their reliable
319 segmentation (Figure 3D, Lipid Droplets in neuronal cells).

320 **Limitations**

321 The protocol relies on the user to define the organelle to be classified, after that the procedure is not user biased. It is,
322 therefore recommended that the classifier is trained by either an experienced researcher or the beginning researcher
323 compares their classifier data to a secondary marker to ensure that the area corresponds to the organelle area of interest
324 (see Figure 2A). Caution should be applied when estimating absolute coverage of organelles. As we show in Figure 2C, it
325 depends on imaging parameters. Quantification of relative coverage, including negative and positive controls is
326 recommended, e.g. organelle abundance between conditions imaged with the same microscopy parameters (e.g. Figure
327 3A).

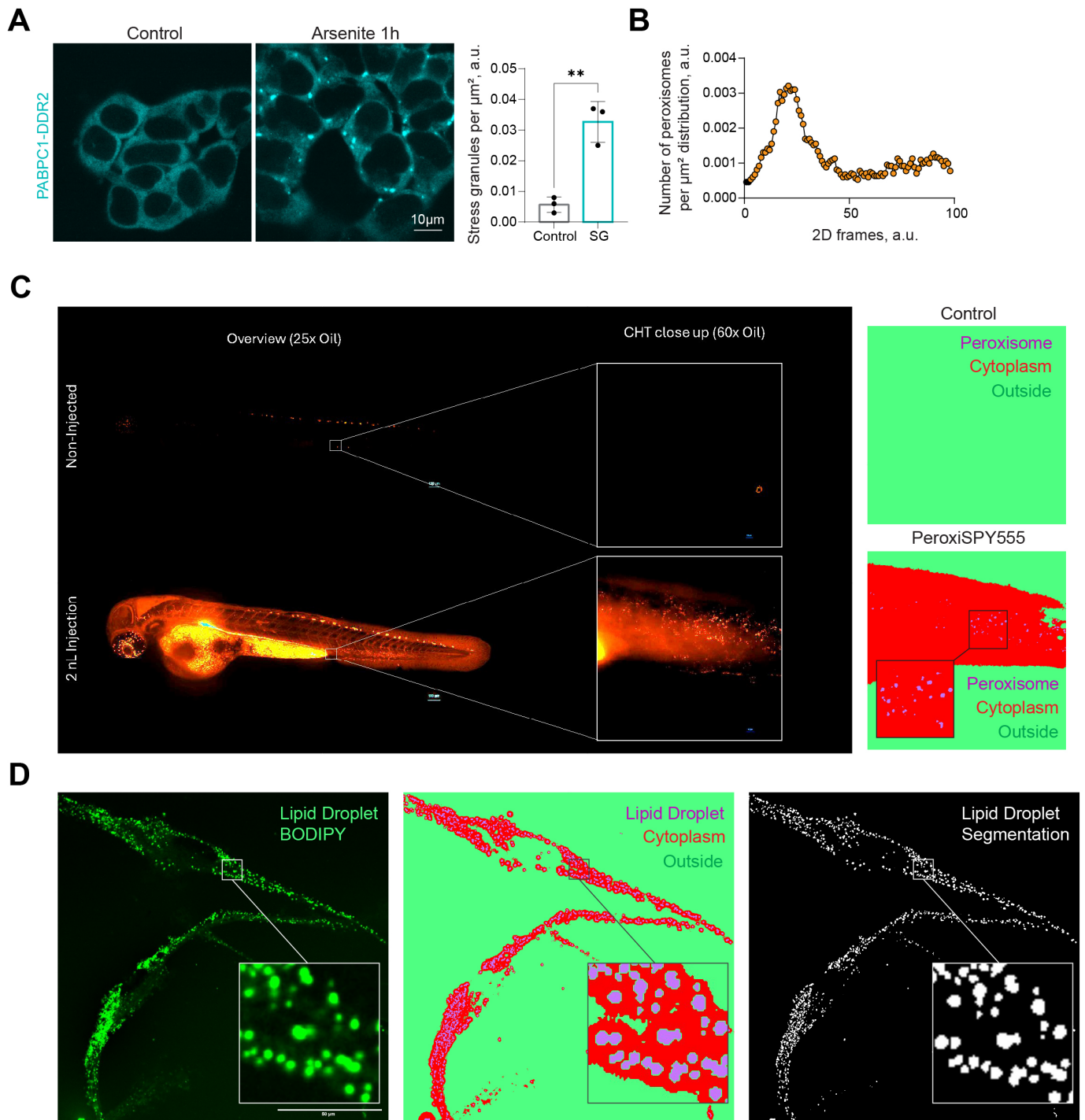
328
329 *To ensure independent validation we provide a dataset to train and apply the classifier (Supplementary dataset S1 that*
330 *includes two images for training and detection), additionally we include the expected results table (Supplementary table S1).*
331

Figure 2. Protocol validation



332
 333 **Figure 2. Protocol validation** A. Confocal microscopy of peroxisomes in HEK293T cells (upper row) expressing
 334 peroxisome marker GFP-SKL, stained with PeroxiSPY (1 μ M for 10 m) or (bottom row) expressing CRISPR/Cas9
 335 PABPC1-DDR2 and stained with PeroxiSPY(1 μ M for 10 m). Segmentation panels (column 4) show areas recognized by
 336 the classifier. Quantification shows the area size detected with the manual threshold method and the area segmented by
 337 classifier, N=3, mean \pm SEM ns – non-significant. **B.** Determination of segmented areas and number of sequential training
 338 loops required for appropriate classifier training. Each dot represents additional training area including the data from the
 339 previous training. **C.** Confocal microscopy of peroxisomes in HEK293T cells stained with PeroxiSPY (1 μ M for 10 m)
 340 imaged with 0.5, 1, or 2% laser power. Quantification shows the area size detected with the classifier trained on laser
 341 power 1% image.
 342
 343

Figure 2. Protocol application



344
 345
 346 **Figure 3. Protocol application A.** Confocal microscopy of stress granules in HEK293T PABPC1-DDR2 cells in control
 347 and 200 μM arsenite (60 m) conditions. Quantification shows the cytoplasmic density of stress granules, $N=3$, mean \pm
 348 SEM. ** - $p<0.01$. **B-C.** Confocal images of zebrafish embryos at 3-day post fertilization injected with 2 nl of
 349 PeroxySpy555 at 1 mM in the blood circulation by the duct of Cuvier. Images were acquired 2 h after injection, using a
 350 W1 Nikon Spinning disk microscope. Images were segmented using macro and peroxisomal areas were detected and
 351 plotted on the histogram (B). (D) Macro-based segmentation of lipid droplets in human iPSC-derived microglia.
 352 Representative fluorescence image of human iPSC-derived microglia at day 21 of differentiation (D21) stained with
 353 BODIPY 493/503 to label lipid droplets. Corresponding WEKA segmentation and binary segmentation mask generated

354 using the custom macro; white indicates segmented lipid droplets and black denotes cytoplasm/background. Scale bars, 50
355 μm .

356
357

358 **General notes and troubleshooting**

359

360 **General notes**

361 1. The classifiers used in this protocol are trained on the data using macro (code S1) and can be used to estimate organelle
362 abundance. The users can also follow the training algorithm to train their own classifier to be applied in different conditions,
363 or for a different cellular compartment.

364 2. The protocol has been tested in several microscope settings (e.g. laser power changes), using several organelle markers.
365 Its applicability to a different organelle needs to be confirmed with a secondary marker as we have done in figure 2.

366 3. It is recommended to train the classifier for 5-10 loops on each dataset (using a representative image) with new microscopy
367 parameters.

368

369 **Troubleshooting**

370

371 Problem 1: Unable to detect organelle areas

372 Possible cause: Image quality is low

373 Solution: Optimize the imaging acquisition parameters. For example, HV (gain) will increase brightness but will also
374 increase noise. Increase laser power and decrease gain to improve the signal-to-noise ratio.

375 Possible cause: photobleaching

376 Solution: Some fluorescent molecules are photostable (e.g. PeroxiSPY), while others can bleach with laser exposure (e.g.
377 DDR2). Reduce light exposure when handling samples by wrapping the plate in aluminum foil or working in the dark room.

378 When imaging, do not image the same area repeatedly. Find the area on a low laser power setting and then switch to the
379 higher laser power setting before acquiring the final image. Use mounting media with an antifade protection if using fixed
380 samples.

381

382 Problem 2: Organelle areas are too big

383 Possible cause: User defined areas are not specific to organelle during the selection process

384 Solution: Select areas strictly within the organelle

385 Possible cause: oversaturation

386 Solution: When setting microscopy parameters avoid saturation by reducing the gain and the laser power until only few or
387 no pixels remain saturated.

388

389 Problem 3: Organelle cluster prevents quantification of the numbers

390 Possible cause: Watershed is not applied during the procedure (point 2.4, type 1 – to apply)

391 Solution: Apply the watershed that separates clusters into separate compartments

392

393 Problem 4: Not enough organelles are visible while training

394 Possible cause: The Randomly selected training area is too small

395 Solution: Navigate to lines 4 and 5 in the macro while it is open in Fiji and not running. Edit lines 4 and 5 in the macro so
396 “w” and “h” variables are larger. For example, lines 4 and 5 could be replaced with:

397 Line 4: “w = 250;”

398 Line 5: “h = 250;”

399

400

401

402

403 Supplementary information

404

405 The following supporting information can be downloaded [here](#) (link available when this protocol is published online):

406 1. Dataset S1. Example images to train and quantify the density of peroxisomes

407 2. Code S1. Macro to quantify organelle abundance

408 3. Table S1. Example output results table.

409 4. Video S1. Video explanation of the workflow.

410

411

412 Acknowledgments

413

414 Specific contributions of each author, Conceptualization, A.J.L. and T.A.; Investigation, A.J.L., D.C., N.H., L.R.,
415 M.S., N.F.C. and T.A. Writing—Original Draft, A.J.L. and T.A.; Writing—Review & Editing, A.J.L., D.C., N.F.C.,
416 N.H., M.S., L.R., S.K. and T.A.; Funding acquisition, S.K. and T.A.; Supervision, N.H., M.S., S.K. and T.A.

417 We thank the School of Biological Sciences Imaging and Microscopy Centre (IMC) for providing access to essential
418 equipment.

419 Funding sources that supported the work: TA was funded by the HFSP Long-term Fellowship (LT000559/2021-L),
420 the University of Southampton, the Wessex Medical Research Innovation Grant, and the European Leukodystrophy
421 Association (ELA International: grant number 2024-017C1A to S.K. and T.A.).

422 The protocol was derived from peroxisome density calculations in (Borisyyuk et al., 2025; Korotkova et al., 2024).

423 We thank David S. Chatelet for providing insights to the Fiji macro language. We thank Prof. Dr. V.M. Heine
424 (Amsterdam UMC and Vrije Universiteit Amsterdam) for providing access to microscopy images of iPSC-derived
425 microglia stained for lipid droplets, which were used for validation.

426 Public forums utilized in the organelle abundance macro: Reddit.com, Image.sc, imagej.273.s1.nabble.com, and
427 ImageJ.net.

428

429 Competing interests

430

431 The authors declare no conflicts of interest.

432

433

434 Ethical considerations

435

436 This protocol does not use human or animal subjects.

437

438 References

439

440 Amen, T., and D. Kaganovich. 2020. Quantitative photoconversion analysis of internal molecular dynamics in stress granules and
441 other membraneless organelles in live cells. *STAR Protoc.* 1:100217.

442 Amen, T., and D. Kaganovich. 2021. Stress granules inhibit fatty acid oxidation by modulating mitochondrial permeability. *Cell*
443 *Reports.* 35.

444 Arganda-Carreras, I., V. Kaynig, C. Rueden, K.W. Eliceiri, J. Schindelin, A. Cardona, and H. Sebastian Seung. 2017. Trainable
445 Weka Segmentation: a machine learning tool for microscopy pixel classification. *Bioinformatics.* 33:2424-2426.

446 Bi, Q., K.E. Goodman, J. Kaminsky, and J. Lessler. 2019. What is Machine Learning? A Primer for the Epidemiologist. *Am J*
447 *Epidemiol.* 188:2222-2239.

448 Borisyyuk, A., C. Howman, S. Pattabiraman, D. Kaganovich, and T. Amen. 2025. Protein Kinase C promotes peroxisome biogenesis
449 and peroxisome-endoplasmic reticulum interaction. *J Cell Biol.* 224.

450 Cunliffe, V. 2003. Zebrafish: A Practical Approach. Edited by C. NÜSSEIN-VOLHARD and R. DAHM. *Genetics Research -*
451 *GENET RES.* 82:79-79.

452 Howman, C., T. Cohen, M.Y. Shlomy, M.S. van Aerle, R.E. Carmichael, M. Schuhmacher, L. Reymond, E. Zalckvar, D.
453 Kaganovich, and T. Amen. 2025. Peroxisome Staining in Mammalian Cells Using Peroxisome-Specific Probes. *J Vis*
454 *Exp.*

455 Isensee, F., P.F. Jaeger, S.A.A. Kohl, J. Petersen, and K.H. Maier-Hein. 2021. nnU-Net: a self-configuring method for deep
456 learning-based biomedical image segmentation. *Nat Methods.* 18:203-211.

- 457 Ivanov, P., N. Kedersha, and P. Anderson. 2019. Stress Granules and Processing Bodies in Translational Control. *Cold Spring*
458 *Harb Perspect Biol.* 11.
- 459 Korotkova, D., A. Borisyuk, A. Guihur, M. Bardyn, F. Kuttler, L. Reymond, M. Schuhmacher, and T. Amen. 2024. Fluorescent
460 fatty acid conjugates for live cell imaging of peroxisomes. *Nat Commun.* 15:4314.
- 461 Kumar, R., M. Islinger, H. Worthy, R. Carmichael, and M. Schrader. 2024. The peroxisome: an update on mysteries 3.0. *Histochem*
462 *Cell Biol.* 161:99-132.
- 463 Lam, V.K., J.M. Byers, M.C. Robitaille, L. Kaler, J.A. Christodoulides, and M.P. Raphael. 2025. A self-supervised learning
464 approach for high throughput and high content cell segmentation. *Commun Biol.* 8:780.
- 465 Lefebvre, A., G. Sturm, T.Y. Lin, E. Stoops, M.P. Lopez, B. Kaufmann-Malaga, and K. Hake. 2025. Nellie: automated organelle
466 segmentation, tracking and hierarchical feature extraction in 2D/3D live-cell microscopy. *Nat Methods.* 22:751-763.
- 467 Metz, J., I.G. Castro, and M. Schrader. 2017. Peroxisome Motility Measurement and Quantification Assay. *Bio Protoc.* 7.
- 468 Newby, J.M., A.M. Schaefer, P.T. Lee, M.G. Forest, and S.K. Lai. 2018. Convolutional neural networks automate detection for
469 tracking of submicron-scale particles in 2D and 3D. *Proc Natl Acad Sci U S A.* 115:9026-9031.
- 470 Protter, D.S.W., and R. Parker. 2016. Principles and Properties of Stress Granules. *Trends Cell Biol.* 26:668-679.
- 471 Riggs, C.L., N. Kedersha, P. Ivanov, and P. Anderson. 2020. Mammalian stress granules and P bodies at a glance. *J Cell Sci.* 133.
- 472 Russell, R.A., N.M. Adams, D.A. Stephens, E. Batty, K. Jensen, and P.S. Freemont. 2009. Segmentation of fluorescence
473 microscopy images for quantitative analysis of cell nuclear architecture. *Biophys J.* 96:3379-3389.
- 474 Schindelin, J., I. Arganda-Carreras, E. Frise, V. Kaynig, M. Longair, T. Pietzsch, S. Preibisch, C. Rueden, S. Saalfeld, B. Schmid,
475 J.Y. Tinevez, D.J. White, V. Hartenstein, K. Eliceiri, P. Tomancak, and A. Cardona. 2012. Fiji: an open-source platform
476 for biological-image analysis. *Nat Methods.* 9:676-682.
- 477 Schneider, C.A., W.S. Rasband, and K.W. Eliceiri. 2012. NIH Image to ImageJ: 25 years of image analysis. *Nat Methods.* 9:671-
478 675.
- 479 Shannon, C.E. 1949. Communication in the Presence of Noise. *Proceedings of the IRE.* 37:10-21.
- 480 Wanders, R.J., and H.R. Waterham. 2006. Biochemistry of mammalian peroxisomes revisited. *Annu Rev Biochem.* 75:295-332.
- 481 Wanders, R.J.A., H.R. Waterham, and S. Ferdinandusse. 2018. Peroxisomes and Their Central Role in Metabolic Interaction
482 Networks in Humans. *Subcell Biochem.* 89:345-365.
- 483